

Dependence of low redshift Type Ia Supernovae luminosities on host galaxies *

Wen-Ke Liang^{1,2,3} and Jian-Cheng Wang^{1,2}

¹ National Astronomical Observatories / Yunnan Observatory, Chinese Academy of Sciences, Kunming 650011, China; lwk@ynao.ac.cn

² Key Laboratory for the Structure and Evolution of Celestial Objects, Chinese Academy of Sciences, Kunming 650011, China

³ University of Chinese Academy of Sciences, Beijing 100049, China

Received 2013 February 4; accepted 2013 May 8

Abstract We study the relation between Type Ia Supernovae (SNe Ia) and properties of their host galaxies using a large sample with low redshift. By examining the Hubble residuals of the entire sample from the best-fit cosmology, we show that SNe Ia in passive hosts are brighter than those in star-forming hosts after light curve correction at the 2.1σ confidence level. We find that SNe Ia in high luminosity hosts are brighter after light-curve correction at the $> 3\sigma$ confidence level. We also find that SNe Ia in large galaxies are brighter after light-curve correction at the $\geq 2\sigma$ confidence level. We demonstrate that the residuals depend linearly on host luminosity at a confidence of 4σ or host size at a confidence of 3.3σ .

Key words: supernovae: general — distance scale — galaxies: classification

1 INTRODUCTION

The use of Type Ia supernovae (SNe Ia) as standard candles in estimating cosmological distances has proven to be indispensable for modern cosmology, leading to the remarkable discovery that the expansion of the Universe is accelerating (Riess et al. 1998; Perlmutter et al. 1999; Kessler et al. 2009; Guy et al. 2010; Suzuki et al. 2012). According to the current theory, the progenitor of an SN Ia is a carbon-oxygen white dwarf that approaches the Chandrasekhar limit, resulting in a thermonuclear explosion (Hillebrandt & Niemeyer 2000; Wang & Han 2012). However, the exact mechanism by which the progenitor accumulates this mass remains uncertain. Investigations of the physical properties of SN Ia host galaxies can provide insight into the environment of the SN Ia progenitor system. Furthermore, although SNe Ia are remarkably standardizable, the corrections for light-curve width and color still result in a scatter in peak brightness of ~ 0.15 mag (Guy et al. 2007; Jha et al. 2007; Conley et al. 2008). The search for the relation between SN Ia luminosity and type of host galaxy will help to reveal the origin of this scatter.

Over the years, several correlations between SNe Ia and the properties of their host galaxies have been discovered. The characteristics, such as morphology, color, star formation rate, metallicity and stellar age of the host galaxy, provide clues to understanding the progenitors. SNe Ia in E/S0

* Supported by the National Natural Science Foundation of China.

galaxies are brighter than those in later-type galaxies after light-curve shape and color corrections are performed (Hicken et al. 2009b). SNe Ia are brighter in massive hosts and hosts with low star formation rate per stellar mass (specific star formation rate) after the maximum brightness of SNe Ia is corrected by using their light-curve shape and color (Sullivan et al. 2010; Kelly et al. 2010; Lampeitl et al. 2010). Gupta et al. (2011) also found that over-luminous SNe Ia tend to occur in older stellar populations after light-curve correction is applied.

However, there is still little research about the correlations between SNe Ia and the properties of their host galaxies at low redshift. In this paper, we investigate correlations between SNe Ia and the properties of their host galaxies at low redshift. If the correlations are identified at a low redshift, host properties such as type, size and luminosity could be combined with light curve parameters to further improve estimates of luminosity distance.

In this paper, we study the relation between luminosities of SNe Ia and properties of their host galaxies, such as type, size and luminosity, by using a larger sample at low redshift. In Section 2, we introduce the sample of SNe Ia and host galaxies, and outline the details of our analysis using the publicly available light curve fitting procedure SALT2 (Guy et al. 2007). We investigate how the widths and colors of light curves from SNe Ia vary with properties of its host galaxy in Section 3. In Section 4, we present the relation between Hubble residuals and light curve parameters, host galaxy type, luminosity and size. The conclusions are presented in Section 5. Throughout we use a flat Λ CDM cosmological model with $\Omega_M = 0.270$ and $H_0 = 70 \text{ km s}^{-1} \text{ Mpc}^{-1}$.

2 SAMPLE AND DATA

2.1 Sample of Low Redshift SNe Ia

To investigate the relationship between SNe Ia and properties of their host galaxies, we choose a sample of low redshift cases. This includes eight main samples: Calán/Tololo (Hamuy et al. 1996, 29 SNe Ia), CfAI (Riess et al. 1999, 22 SNe Ia), CfAII (Jha et al. 2006, 44 SNe Ia), CfAIII (Hicken et al. 2009a, 185 SNe Ia), LOSS (Ganeshalingam et al. 2010, 165 SNe Ia) CSP (Contreras et al. 2010, 35 SNe Ia), CSPII (Stritzinger et al. 2011, 50 SNe Ia) and CfAIV (Hicken et al. 2012, 94 SNe Ia). For the Calán/Tololo, CfAI, CfAII and LOSS samples, the data were transformed by the authors from the natural instrumental system into the Landolt (1992) system using linear transformations derived from stars in a limited color range. For the CfAIII, CSP, CSPII and CfAIV samples, natural system photometry was used in our analysis, and we disregarded the U band because of its relatively large error.

2.2 Selection of SNe

We exclude 150 repeated SNe Ia and 29 known peculiar SNe Ia by hand, such as SN 2000cx. Because of the potential issue of a discontinuous step in the local expansion rate (Hubble bubble) detected by Jha et al. (2007), we choose the cut at $z = 0.010$ (Conley et al. 2011).

For a reliable cut in the light-curve data, we will select SNe Ia according to the following requirements from the available phases $\tau = (T_{\text{obs}} - T_{\text{max}})/(1+z)$ of photometric observations, where T_{obs} is the date of observation for the light-curve data, and T_{max} is the date of the light maximum:

- (i) Measurements at five different epochs or more are in the range $\tau < +60$ days.
- (ii) At least two measurements are in the range $\tau < +6$ days.

We discard SNe Ia without reliable light-curve parameters as computed by the SALT2 light-curve fitter. The Galactic reddening along the line of sight should satisfy $E(B - V)_{MW} < 0.5$ mag because the assumed Galactic value of $R_V = 3.1$ is not appropriate for highly extinguished objects. Next, we take the stretch parameter to be $-4 < x_1 < 3$ for SALT2 and the color to be $-0.2 < c <$

Table 1 Selection of SNe Ia from Low Redshift Samples

| Sample | Initial ¹ | Unreliable ² | <i>z</i> Cut | <i>x</i> ₁ | Color | Outliers | Final ³ |
|--------------|----------------------|-------------------------|--------------|-----------------------|-------|----------|--------------------|
| Calán/Tololo | 28 | 9 | 0 | 0 | 0 | 0 | 19 |
| CfA1 | 21 | 5 | 6 | 0 | 1 | 0 | 9 |
| CfA2 | 24 | 12 | 2 | 0 | 0 | 0 | 10 |
| CfA3 | 87 | 50 | 0 | 1 | 2 | 0 | 34 |
| CfA4 | 74 | 37 | 2 | 0 | 0 | 1 | 34 |
| CSP1 | 21 | 3 | 3 | 2 | 1 | 0 | 12 |
| CSP2 | 40 | 4 | 4 | 0 | 3 | 1 | 28 |
| LOSS | 150 | 26 | 21 | 0 | 8 | 0 | 95 |
| all | 445 | 146 | 38 | 3 | 15 | 2 | 241 |

The number of SNe Ia removed by each selection criterion. Many SNe Ia fail multiple cuts.

¹ The initial number of SNe Ia, after the removal of known peculiar SNe Ia, SNe Ia with clear photometric inconsistencies, and SNe Ia with better photometry from other samples.

² SNe Ia with unreliable data due to an insufficient number of epochs or high Milky Way $E(B - V)$.

³ The number of SNe Ia satisfying all selection criteria.

Table 2 Properties of Host Galaxies in samples of SNe Ia

| Sample | SALT2 output ¹ | Star-forming | AGN | Passive | Three types ² | Diameter/magnitude ³ |
|--------------|---------------------------|--------------|-----|---------|--------------------------|---------------------------------|
| Calán/Tololo | 19 | 0 | 1 | 0 | 1 | 1 |
| CfA1 | 9 | 0 | 1 | 2 | 3 | 8 |
| CfA2 | 10 | 0 | 1 | 1 | 2 | 5 |
| CfA3 | 34 | 5 | 4 | 6 | 15 | 20 |
| CfA4 | 34 | 2 | 3 | 5 | 10 | 18 |
| CSP1 | 12 | 3 | 1 | 2 | 6 | 8 |
| CSP2 | 28 | 4 | 2 | 4 | 10 | 14 |
| LOSS | 95 | 7 | 9 | 11 | 27 | 58 |
| all | 241 | 21 | 22 | 31 | 74 | 132 |

¹ The number of SNe Ia using SALT2, after all of the selection criteria in the last section are applied.

² The sum of three types of galaxies: star-formings, AGNs and passives.

³ Galaxies which have magnitude or size data.

0.4. We exclude SN 2008cm and SN 2006bd due to 3σ intrinsic luminosity dispersions in the best-fit cosmology. The data on SNe Ia can be obtained online. The results of all these selections are shown in Table 1.

2.3 Properties of the Host Galaxy

Our main host galaxy data are from Hakobyan et al. (2012). We switch the g -band apparent magnitude of the host galaxy into absolute magnitude. K-correction is given by Equation (1), and the value of the second item is about 0.1 mag at $z \sim 0.1$ and about 0.05 mag at $z \sim 0.05$. In our sample, only one galaxy has a redshift above 0.1 and the majority (92.5%) of these host galaxies have ≤ 0.05 . Therefore we only consider the first K-correction to compute absolute magnitude, e.g.,

$$K = 2.5 \log(1 + z) + 2.5 \log \frac{\int_{\lambda_1}^{\lambda_2} I(\lambda) \phi_\lambda d\lambda}{\int_{\lambda_1}^{\lambda_2} I(\frac{\lambda}{1+z}) \phi_\lambda d\lambda}. \tag{1}$$

Regarding galaxy sizes, we use the g -band diameters measured at the isophotal level of $\mu_g = 25$ mag arcsec⁻². In Figure 1, we show the relation between the size of the g -band and absolute magnitude. Table 2 lists the properties of host galaxies in terms of the SN Ia samples.

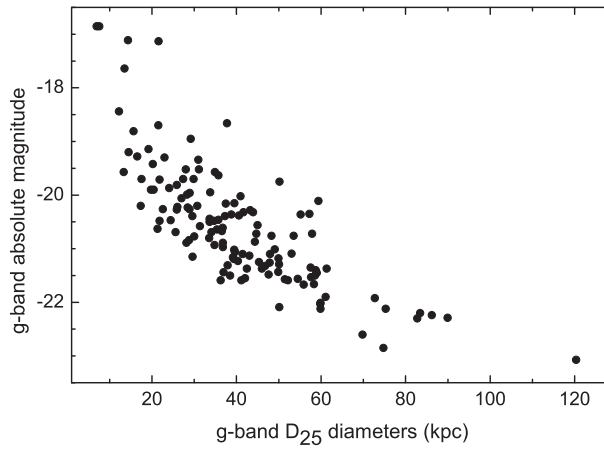


Fig. 1 The relation between galaxy size and absolute magnitude.

To examine the dependence of SN Ia properties on environmental conditions, we classify the SN Ia hosts into different groups. According to the active extent of host galaxies, we take the measures of Hakobyan et al. (2012) who used the WHAN diagram to separate host galaxies into three subsamples: star-forming galaxies, Active Galactic Nuclei (AGNs) and passive galaxies. The second split is performed according to their luminosity: galaxies with g -band magnitude ≤ -20.75 mag are classified as high luminosity, and those with g -band magnitude > -20.75 mag as low luminosity. The third split is based on host size: galaxies with $\mu_g = 25$ mag arcsec $^{-2}$ diameters ≤ 37.5 kpc are small, but others are large. The exact values chosen as the split points are a somewhat subjective choice. The split points for luminosity and size are both chosen to separate the hosts into bins of approximately equal sizes (we consider the effect of varying the last two split points in later sections).

3 CORRELATIONS WITH SN FIT PARAMETERS

SALT2 reports a corrected B -band peak apparent magnitude (m_B^{corr}), a stretch value (x_1) and a color (or c) term for each individual SN. They have a relation of

$$m_B^{\text{corr}} = m_B + \alpha x_1 - \beta c, \quad (2)$$

where α describes the overall stretch law for the sample and β is the color law for the whole sample; m_B and c are only corrected for Milky Way extinction without host galaxy extinction. α and β are typically determined from simultaneous fits with the cosmological parameters.

3.1 Extent of the Active Host

In Figure 2, we show the output of SALT2 (x_1 and c values) according to extent of the active host galaxy. The solid (blue) triangles denote SNe Ia in star-forming galaxies, the solid (green) squares indicate SNe Ia in AGNs, and the solid (red) circles show SNe Ia in passive galaxies. The distribution of x_1 is obviously different.

In Table 3, we show the mean values and standard deviations about x_1 and c . In agreement with the results given by Lampeitl et al. (2010), we confirm that SNe Ia present a clear difference in the x_1 distributions, and SNe Ia with small x_1 favor passive galaxies, while SNe Ia with large x_1 favor star-forming galaxies. Using the t-test, we find that the mean value of x_1 in star-forming galaxies

Table 3 Statistical Values of SN Fitting Parameters for Host Galaxy Types

| Galaxy Type | N | Mean (x_1) | Std Dev (x_1) | Mean (c) | Std Dev (c) |
|--------------|-----|----------------|-------------------|--------------|-----------------|
| Star Forming | 21 | 0.404 | 0.842 | 0.038 | 0.123 |
| AGN | 22 | -0.261 | 0.865 | 0.021 | 0.134 |
| Passive | 31 | -0.737 | 1.265 | 0.007 | 0.010 |

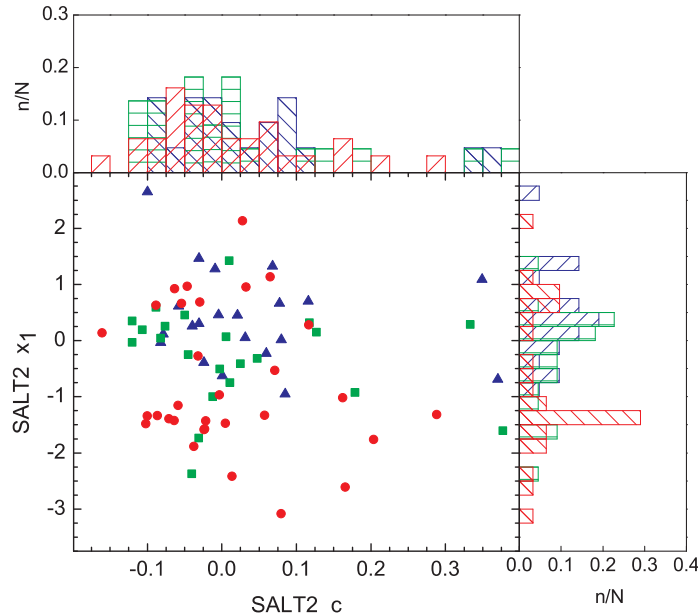


Fig. 2 The observed distribution of x_1 and c (color) values for the extent of active hosts. Blue solid triangles indicate SNe Ia in star-forming galaxies, green solid squares indicate SNe Ia in AGNs, and red solid circles denote SNe Ia in passive galaxies. The histograms in the top panel of the figure show the normalized distribution of c for star-forming galaxies (*blue*), AGNs (*green*) and passive galaxies (*red*). The right panel shows the histograms of x_1 for different host galaxies.

is significantly larger than that in other types of galaxies, with passive galaxies at a confidence of 4σ , and with AGNs at a confidence level of 2.7σ . However the mean value of x_1 is not obviously different in AGNs and passive galaxies.

From Figure 2, we note that there is no relation between the color term (c) of SNe Ia and type of host galaxy. For the t-test, at the 2σ confidence level, there is no significant difference in c values for the three types of host galaxies, implying that the rest-frame colors of SNe Ia are dominated by either local, circumstellar dust with the same color distributions, or by variations of the same intrinsic color in all galaxy types.

3.2 Host Luminosity

In Figure 3, we show the dependence of the output of SALT2 (x_1 and c) on absolute magnitudes of the host in the g -band. At about the 2σ confidence level, we find that SNe Ia with a smaller x_1 tend

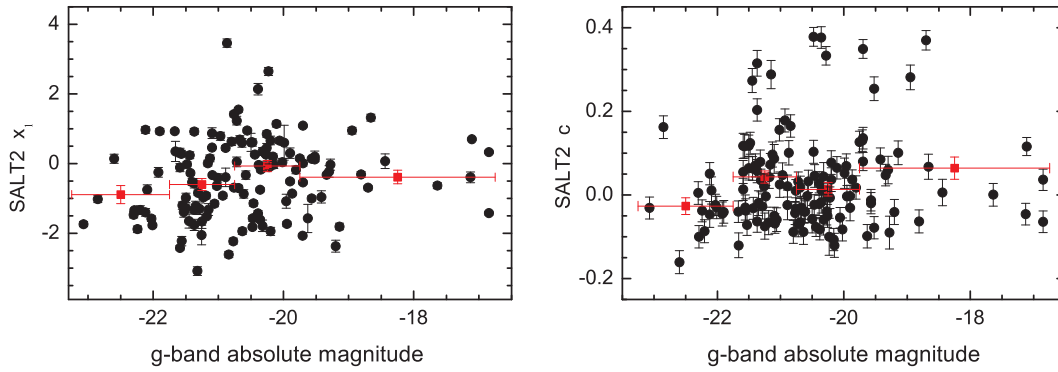


Fig. 3 The left panel shows the dependence of observed x_1 on g -band absolute magnitudes. The square bins represent the mean value of x_1 in each bin. The right panel is similar to the left one but for c .

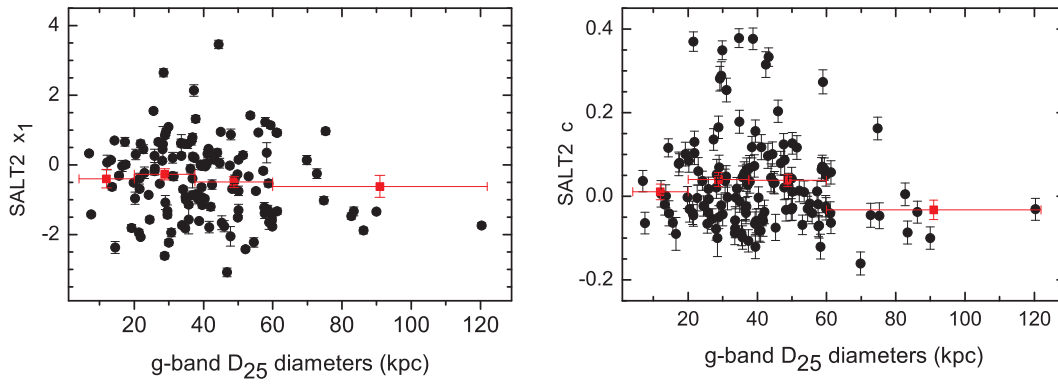


Fig. 4 Same as Fig. 3, but for size instead of luminosity.

to be found in host galaxies that have a high luminosity. However, at the 2σ confidence level, there is no correlation between absolute magnitude of the host and c .

3.3 Size of the Host

In Figure 4, we show the output of SALT2 (x_1 and c) with hosts that have different sizes. At the 2σ confidence level, there is no correlation between x_1 and size of the host, and c is also not correlated with this quantity.

4 RESIDUALS FROM GLOBAL COSMOLOGICAL FITS OF HOST GALAXIES

We now perform a χ^2 fit with the equation

$$\chi^2 = \sum_N \frac{(m_B^{\text{corr}} - m_B^{\text{mod}}(z, \mathcal{M}_B; \Omega_M))^2}{\sigma_{\text{stat}}^2 + \sigma_{\text{int}}^2}, \quad (3)$$

where m_B^{corr} is given by Equation (2) and m_B^{mod} is the B -band magnitude of the cosmological model for each SN Ia given by

$$m_B^{\text{mod}} = 5 \log_{10} \mathcal{D}_L(z; \Omega_M) + \mathcal{M}_B. \quad (4)$$

\mathcal{D}_L is the reduced luminosity distance. $\mathcal{M}_B = M_B + 5 \log_{10}(c/H_0) + 25$, where M_B is the absolute magnitude of an SN Ia in the B -band. For the SALT2 fitter, M_B is given under $x_1 = 0$ and $c = 0$. For convenience, we present our results as M_B rather than \mathcal{M}_B , but it is noted that H_0 is taken as $70 \text{ km s}^{-1} \text{ Mpc}^{-1}$.

σ_{int} parameterizes the intrinsic dispersion of each SN Ia, and the sum is over N SNe Ia entering the fit. σ_{stat} is the total identified statistical error and includes the uncertainties in m_B , m_B^{mod} and peculiar velocity that is set as 400 km s^{-1} in this paper.

One way is to examine the residuals of SNe Ia from the cosmological fit using the entire sample at low redshift; Ω_M is set as 0.270. Throughout, we define a Hubble residual (HR) as $\text{HR} = m_B^{\text{corr}} - m_B^{\text{mod}}$, implying that after light-curve correction is applied, brighter SNe Ia have negative Hubble residuals.

We use Alex Conley's `minuit_cosfitter`¹ code to do χ^2 cosmological fitting for the entire sample that has 241 SNe Ia. We assume an intrinsic dispersion of $\sigma_{\text{int}} = 0.12 \text{ mag}$ that adds error to the distance modulus to compute a reduced χ^2 close to one (i.e., $\chi^2/\text{ndf} \approx 1$). We get the nuisance parameters of $(M_B, \alpha, \beta) = (-19.080, 0.148, 3.059)$, shown in Table 4.

Table 4 Best Fitting Values for M_B , α , β and rms

| α | β | M_B | rms | N | χ^2 |
|-------------------|-------------------|---------------------|-------|-----|----------|
| 0.148 ± 0.012 | 3.059 ± 0.116 | -19.080 ± 0.013 | 0.196 | 241 | 240.2 |

We use the best-fit cosmological results of the entire sample to derive new subsamples according to properties of the host galaxy, such as a subsample of host types (74 SNe Ia), a subsample of host absolute magnitudes (132 SNe Ia) and a subsampe of host sizes (132 SNe Ia).

4.1 Extent of Active Hosts

In Table 5, we show the residuals of different host galaxies. We apply a t-test to the residuals from different host galaxies. At 2.1σ confidence, the residuals in passive galaxies are more negative than those in star-forming galaxies. However, at 2σ confidence, there is no significant difference in the residuals between AGNs and any other galaxies.

Table 5 Statistical Values of Hubble Residuals for Host Galaxy Types

| Galaxy Type | N | Mean | Std Dev |
|--------------|-----|--------|---------|
| Star Forming | 21 | 0.055 | 0.158 |
| AGN | 22 | 0.024 | 0.172 |
| Passive | 31 | -0.035 | 0.186 |

4.2 Host Luminosity

In Table 6, we show the residuals of two luminosity groups and the effect of different split points. At the $>3\sigma$ significance level, the residuals in hosts with high luminosity are more negative than those in hosts with low luminosity, implying that SNe Ia in high luminosity galaxies are brighter than those in high luminosity hosts.

¹ <http://casa.colorado.edu/~aacconley/Software.html>

Table 6 Statistical Values of Hubble Residuals for Absolute Magnitude of Host in the g -band

| Luminosity split M_g | High luminosity hosts | | | Low luminosity hosts | | | Significance ¹ |
|---------------------------|-----------------------|--------|---------|----------------------|-------|---------|---------------------------|
| | N | Mean | Std Dev | N | Mean | Std Dev | |
| -20.25 | 90 | -0.026 | 0.188 | 42 | 0.095 | 0.214 | 3.2 σ |
| -20.5 | 73 | -0.044 | 0.187 | 59 | 0.083 | 0.205 | 3.8 σ |
| -20.75 | 62 | -0.055 | 0.187 | 70 | 0.072 | 0.201 | 3.9 σ |
| -21 | 52 | -0.060 | 0.184 | 80 | 0.059 | 0.204 | 3.6 σ |
| -21.25 | 39 | -0.077 | 0.196 | 93 | 0.050 | 0.197 | 3.5 σ |

¹This shows the significance level where SNe Ia in high luminosity hosts are brighter than those in low luminosity hosts.

Here, we also fit a linear dependence for residuals on absolute magnitude of the host in the g -band or size using the package LINMIX (Kelly 2007), which was used to determine the significance of trends in residuals by Kelly et al. (2010). LINMIX is a Bayesian approach for linear regression using a Markov Chain Monte Carlo (MCMC) analysis, assuming that the measurement errors are Gaussian. We make the assumption that our errors on Hubble residuals are Gaussian and input them into LINMIX; the average of the upper and lower 1σ uncertainties is taken as the error in the dependent variable.

The residuals with absolute magnitudes of the host in the g -band are shown in the left panel of Figure 5. The overplotted lines are the best-fit model determined from LINMIX. In all our LINMIX analyses, we use 10 000 MCMC realizations. For the residuals related to absolute magnitudes, we obtain the best-fit relation

$$\text{HR} = (0.066 \pm 0.015) \times M_g - 1.413 \pm 0.290. \quad (5)$$

The MCMC realizations in LINMIX are used to generate a sampling of the posterior distribution on the slope. Among the MCMC realizations, the slope is greater than zero for nearly 100%. Fitting a Gaussian to the posterior distribution of slope, we yield a mean of 0.066 and a standard deviation of 0.015. From the Gaussian fit, the mean slope does not equal zero at the 4σ confidence level, implying that there is a correlation between the g -band absolute magnitude and the residual.

4.3 Host Size

The statistical values of the residuals and the effect of the different split points in luminosity are shown in Table 7. At the $\geq 2\sigma$ confidence level, the residuals in large hosts are more negative than those in small hosts, implying that SNe Ia in large galaxies are brighter.

Table 7 Statistical Values of Hubble Residuals for Host Size

| Size split D_{25} | Large hosts | | | Small hosts | | | Significance ¹ |
|------------------------|-------------|--------|---------|-------------|-------|---------|---------------------------|
| | N | Mean | Std Dev | N | Mean | Std Dev | |
| 30 | 90 | -0.010 | 0.204 | 42 | 0.058 | 0.197 | 2.1 σ |
| 35 | 78 | -0.024 | 0.197 | 54 | 0.065 | 0.205 | 2.7 σ |
| 37.5 | 67 | -0.015 | 0.177 | 65 | 0.040 | 0.227 | 2 σ |
| 40 | 58 | -0.025 | 0.184 | 74 | 0.042 | 0.215 | 2.2 σ |
| 45 | 44 | -0.031 | 0.180 | 88 | 0.034 | 0.213 | 2.1 σ |

¹This shows the significance level where SNe Ia in large hosts are brighter than those in small hosts.

In the right panel of Figure 5, we plot the residuals with size of host galaxy and give a best-fit relation

$$\text{HR} = (-0.0032 \pm 0.0009) \times D_{25} + 0.138 \pm 0.040, \quad (6)$$

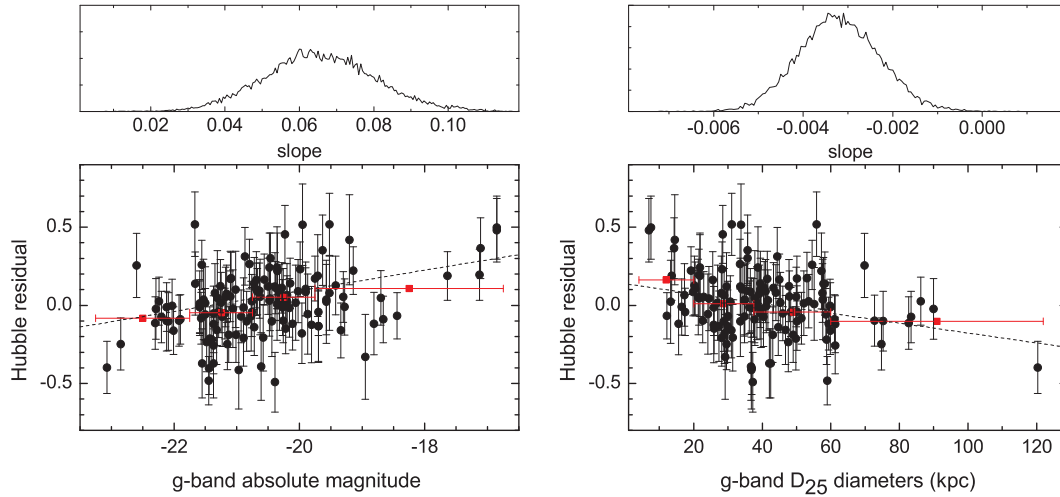


Fig. 5 The left panel in the figure shows the residuals with g -band absolute magnitudes. The right panel shows the residuals with host diameters at $\mu_g = 25 \text{ mag arcsec}^{-2}$. The square bins represent the mean value of residuals in each bin. The overplotted line shows the best fit to all data points as described in Sections 4.2 and 4.3.

where D_{25} represents size in the g -band. Among the MCMC realizations, there is a negative non-zero slope at the 3.3σ confidence level.

5 CONCLUSIONS

In this paper we have examined the photometric properties of SNe Ia in different host galaxies using samples with low redshift from literature. We summarize the main conclusions of the paper as follows.

We confirm, to high significance, a strong correlation between extent and type of the host galaxy and the observed width of the light curve, i.e., small x_1 favors passive host galaxies, but large x_1 favors star-forming galaxies. There is no significant difference for x_1 in AGNs and other galaxies. No significant difference of c appears in three types of hosts. We find that, at about 2σ confidence, smaller x_1 tends to occur in hosts with high luminosity. However, at 2σ confidence, host luminosity is not correlated with c , and host size is also not correlated with x_1 or c .

At 2.1σ confidence, the residuals in passive galaxies are more negative than those in star-forming galaxies. This result is consistent with what was found by Lampeitl et al. (2010) at median redshift. We infer that the correlation between SNe Ia luminosities and their host types could not vary with redshift. At the $>3\sigma$ confidence level, the residuals in high luminosity hosts are more negative. We also find that, at the $>2\sigma$ confidence level, SNe Ia have more negative residuals in large hosts.

Using LINMIX, we find that there is a relation between the residual and host g -band absolute magnitude at the 4σ confidence level, implying that over-luminous SNe Ia easily appear in high luminosity galaxies. Regarding the relation between the residual and host size, the LINMIX fitting shows that there is a negative non-zero slope at the 3.3σ confidence level, which is higher than 2.6σ given by Kelly et al. (2010).

In a larger sample of SNe Ia with low redshift, we find that luminosity of SNe Ia changes with properties of host galaxies, including host type, luminosity and size.

Acknowledgements We would like to thank Alex Conley and Mark Sullivan for their significant help during the course of this research. We thank the CfA Supernova Group, the Carnegie Supernova Project (CSP) and other authors for providing SN Ia data. This research has also used the NASA/IPAC Extragalactic Database (NED) and SIMBAD Astronomical Database. We also thank A. A. Hakobyan for providing data on host galaxies. We acknowledge financial support from the National Basic Research Program of China (973 Program, 2009CB824800), the National Natural Science Foundation of China (Grant Nos. 11133006, 11163006 and 11173054), and the Policy Research Program of Chinese Academy of Sciences (KJ CX2-YW-T24).

References

- Conley, A., Guy, J., Sullivan, M., et al. 2011, *ApJS*, 192, 1
Conley, A., Sullivan, M., Hsiao, E. Y., et al. 2008, *ApJ*, 681, 482
Contreras, C., Hamuy, M., Phillips, M. M., et al. 2010, *AJ*, 139, 519
Ganeshalingam, M., Li, W., Filippenko, A. V., et al. 2010, *ApJS*, 190, 418
Gupta, R. R., D'Andrea, C. B., Sako, M., et al. 2011, *ApJ*, 740, 92
Guy, J., Astier, P., Baumont, S., et al. 2007, *A&A*, 466, 11
Guy, J., Sullivan, M., Conley, A., et al. 2010, *A&A*, 523, A7
Hakobyan, A. A., Adibekyan, V. Z., Aramyan, L. S., et al. 2012, *A&A*, 544, A81
Hamuy, M., Phillips, M. M., Suntzeff, N. B., et al. 1996, *AJ*, 112, 2408
Hicken, M., Challis, P., Jha, S., et al. 2009a, *ApJ*, 700, 331
Hicken, M., Challis, P., Kirshner, R. P., et al. 2012, *ApJS*, 200, 12
Hicken, M., Wood-Vasey, W. M., Blondin, S., et al. 2009b, *ApJ*, 700, 1097
Hillebrandt, W., & Niemeyer, J. C. 2000, *ARA&A*, 38, 191
Jha, S., Kirshner, R. P., Challis, P., et al. 2006, *AJ*, 131, 527
Jha, S., Riess, A. G., & Kirshner, R. P. 2007, *ApJ*, 659, 122
Kelly, B. C. 2007, *ApJ*, 665, 1489
Kelly, P. L., Hicken, M., Burke, D. L., Mandel, K. S., & Kirshner, R. P. 2010, *ApJ*, 715, 743
Kessler, R., Becker, A. C., Cinabro, D., et al. 2009, *ApJS*, 185, 32
Lampeitl, H., Smith, M., Nichol, R. C., et al. 2010, *ApJ*, 722, 566
Landolt, A. U. 1992, *AJ*, 104, 340
Perlmutter, S., Aldering, G., Goldhaber, G., et al. 1999, *ApJ*, 517, 565
Riess, A. G., Filippenko, A. V., Challis, P., et al. 1998, *AJ*, 116, 1009
Riess, A. G., Kirshner, R. P., Schmidt, B. P., et al. 1999, *AJ*, 117, 707
Stritzinger, M. D., Phillips, M. M., Boldt, L. N., et al. 2011, *AJ*, 142, 156
Sullivan, M., Conley, A., Howell, D. A., et al. 2010, *MNRAS*, 406, 782
Suzuki, N., Rubin, D., Lidman, C., et al. 2012, *ApJ*, 746, 85
Wang, B., & Han, Z. 2012, *New Astron. Rev.*, 56, 122